Two-step Thermal Spin Transition and LIESST relaxation of the Polymeric spin crossover compounds $Fe(X\text{-}py)_2[Ag(CN)_2]_2$ (X = H; 3-methyl; 4-methyl; 3,4-dimethyl; 3-Cl)

J. A. Rodríguez-Velamazán,*[a] C. Carbonera,[a,b] M. Castro,[a] E. Palacios,[a] T. Kitazawa,[c] J. F. Létard,[b] R. Burriel[a]

[a] Dr. J. Alberto Rodríguez-Velamazán, Dr. Chiara Carbonera, Dr. Miguel Castro, Dr. Elías Palacios, Prof. Dr. Ramón Burriel.
Instituto de Ciencia de Materiales de Aragón (ICMA)
CSIC - Universidad de Zaragoza, 50009 Zaragoza (Spain)
E-mail: jarv@unizar.es

[b] Dr. Chiara Carbonera, Prof. Dr. Jean-François Létard
Laboratoire des Sciences Moléculaires
Institut de Chimie de la Matière Condensée de Bordeaux (ICMCB)
CNRS UPR No 9048, 33608 Pessac (France)

[c] Prof. Dr. Takafumi Kitazawa
Department of Chemistry, Faculty of Science
Toho University
Miyama, Funabashi, Chiba, 274-8510, (Japan)

This is the pre-peer reviewed version of the following article: Chem.Eur.J.2010,16,8785–8796, which has been published in final form at [http://onlinelibrary.wiley.com/doi/10.1002/chem.201000433/full].

Keywords: Iron(II), Spin Crossover, Magnetic Properties, Calorimetry, Photomagnetism, Mössbauer, Reflectivity.

Abstract

Following the synthesis of a new series of polymeric spin crossover compounds, $Fe(X\text{-}py)_2[Ag(CN)_2]_2$ (py = pyridine, X = H; 3-Cl; 3-methyl; 4-methyl; 3,4-dimethyl), a wide physical characterization including magnetic and calorimetric measurements has revealed that the conversion from the high spin state (HS) to the low spin state (LS) occurs following two-step transitions for three out of five members of the family (X = H, 4-methyl and 3,4-dimethyl). The two other compounds, 3-Cl and 3-methyl, show respectively an incomplete spin transition and no transition at all, remaining in the HS state in the whole temperature range. The spin crossover behaviour, when it occurs, is well described using a thermodynamic model that considers both steps. The calculations using this model show the low cooperativity in this type of systems. Reflectivity and photomagnetic experiments reveal that all the compounds (except 3-methyl) undergo light-induced excited spin state trapping (LIESST) at low temperatures. Isothermal HS to LS relaxation curves at different temperatures support the low cooperativity character, following an exponential decay law, although in the thermally activated regime and for the X = H and 3,4-dimethyl compounds the behaviour is well described using a double exponential function in accordance with the two step thermal spin transition. The thermodynamic parameters determined from this isothermal analysis are used for the simulation of the thermal relaxation curves, that nicely reproduce the experimental data.

Introduction

Materials that undergo variation of their physical properties under external perturbations, like temperature, light, pressure, electric and magnetic fields are potential candidates to applications in the field of information storage devices, molecular switches and sensors. Spin crossover (SCO) compounds, most commonly Fe(II) complexes, where the spin state of the transition metal can be switched in a controlled manner between low spin (LS) and high spin (HS) states, belong to this class of materials.[1,2]

The interaction with light has attracted remarkable attention since in 1984 the called LIESST effect (Light-Induced Excited Spin State Trapping) was discovered.[3] The irradiation of the SCO compound at low temperature with precise wavelengths, induces a metastable HS state from the LS one. The latter can be subsequently recovered either by the so-called reverse LIESST effect, which occurs if a new irradiation at a different wavelength is performed, or by thermal relaxation if the temperature of the sample is sufficiently increased. Since this last process depends of the heating rate, a characteristic temperature,[4] called T(LIESST), has been experimentally defined to describe the stability of the induced HS state. A systematic study has shown a correlation between the temperature corresponding of the HS - LS thermal transition, $T_{1/2}$, and T(LIESST) (which is estimated from the maxima of the d(χT)/dT curve, being χ the magnetic susceptibility and T the temperature). [4]

Strong intermolecular interactions between SCO metal centres give rise to a cooperative behaviour affecting significantly the thermal spin transition (increasing its abruptness and hysteresis), the LIESST effect and the relaxation process. One of the routes for the cooperativity enhancement is the polymeric approach[5] in which the switching sites are linked by chemical bridges into extended or polymeric structures with varying dimensionality and topology.[6] The number of examples of polymeric compounds where the LIESST effect has been studied is rather low compared with other types of spin-crossover compounds.[7,8]

Along this approach, SCO Hofmann-like clathrate polymeric compounds, in which the metal centres are linked with cyanometalate complexes, have been intensively investigated. The first compound, $Fe(py)_2[Ni(CN)_4]$ (py = pyridine), synthesized by Kitazawa in 1996,[9], shows a two dimensional (2D) structure and a cooperative spin transition. Substitutions in the py ligand[10] give rise to different magnetic behaviours including incomplete gradual or cooperative transitions and even two-step spin transitions induced by pressure.[11,12]. The LIESST effect has not been reported for these compounds.

A main part of the recent works has been performed by the group of Prof. J. A. Real. The use of different ligands and cyanide complexes gives rise to 2D and 3D interpenetrated networks and architectural isomerism with different magnetic behaviours. So, for example the 2D $Fe(pmd)_2[Cu(CN)_2]_2$ (pmd = pyrimidine)[7e] compound undergoes both a complete cooperative thermal spin transition at around 140 K and LIESST conversion (T(LIESST) = 73 K). If Ag instead of Cu is used, two 3D polymorphs of $Fe(pmd)_2[Ag(CN)_2]_2$ are obtained[13] and also a 3D topology is obtained for $Fe(3\text{-}CNpy)_2[M(CN)_2]_2 \cdot nH_2O$ (M = Ag, Au),[14] with three supramolecular isomers showing different magnetic behaviours. To our knowledge, photomagnetic studies have not been performed for these systems. In contrast, while the LIESST effect has not been reported, an interesting photoswitching around room temperature between LS and HS state has been induced by a laser pulse in the hysteresis loop of the thermal spin transition for the Pt compound[15] of the 3D polymeric family $Fe(pz)_2[M(CN)_4]$ nH_2O (pz = pyrazine, M = Ni, Pd, Pt) [16]. Moreover, a new family, $[Fe(azpy)[M(CN)_4]\cdot nH_2O$ with azpy = 4,4'-azopyridine and M = Ni, Pd, Pt, has been reported [17] as polycrystalline bulk

samples and thin films on gold substrates. They show a 3D structure and spin transitions at temperature higher than 150 K depending on the transition metal ion and on the water content. The LIESST effect has been also detected (but not deeply studied) in all of them except for the powder Ni sample.

A high structural complexity is reached for the $\{Fe(pmd)[Ag(CN)_2)][Ag_2(CN)_3]\}$ [7d] system with a self-interpenetrated 3D polymeric structure, showing a two-step spin transition and photomagnetic behaviour explained by the presence of five crystallographically different iron atoms. The bimetallic doubly interpenetrated 3D complexes $[Fe(L)_x[Ag(CN)_2]_2]\cdot G$, show LS and HS state in the whole temperature range respectively for L = pz (x=1, G = pz) and L = 4,4´-bipyridine (x=2). Nevertheless, for L = bispyridylethylene (x=2), a strong cooperative spin transition with a hysteresis of 95 K and a *T*(LIESST) of about 71 K are detected. [18]

Recently we have reported the 2D spin crossover polymeric compound $Fe(py)_2[Ag(CN)_2]_2$, [19] which undergoes a two-step spin transition. The powder X-ray diffraction data and Mössbauer spectroscopy revealed the existence of only one Fe(II) site at room temperature and that, on lowering temperature, no crystallographic phase transition goes along with the two-step spin transition. However, a large increase of the average thermal factor at the plateau is detected and seems to be compatible with a disordered distribution of spin state.

Centring our attention in this last type of compound, halogen substitution, $Fe(3\text{-}Xpy)_2[M(CN)_2]_2$ (X= F, Cl, Br, I and M= Ag, Au) has been reported [20,21]. They show similar structures constituted of stacks of 2D coordination polymers organized by pairs. All the gold derivatives are HS in the whole temperature range except the 3-Fpy which undergoes a half-spin transition around 140 K with a small hysteresis of 5 K, although under pressure (0.18-0.26 GPa) it reaches a complete two-step spin transition. Additionally a structural transition accompanying the thermal spin transition creates two crystallographically independent Fe(II) sites. In the case of the silver compounds, only the 3Fpy and 3Clpy show a spin transition. For the former one, a low cooperative two step transition takes place, with $T_{1/2}$ (step1) = 162 K and $T_{1/2}$ (step2) = 96 K (due to the presence of two crystallographically distinct Fe(II) sites) and an incomplete transition at $T_{1/2}$ = 106 K (only one Fe(II) site and 50% of conversion) is shown by the latter one. However, the 3Brpy and 3Ipy derivatives remain in the HS state in the whole temperature range. The expected decrease of the ligand field (and therefore decrease of $T_{1/2}$) as the electronegativity of the ligand Xpy increases has not been observed and the behaviour can be explained considering an attenuation of the lattice pressure as the polarizability of the halogen atom is higher. The LIESST effect has not been studied.

In this work, we report the magnetic, photomagnetic, calorimetric, Mössbauer and reflectivity studies of the $Fe(X\text{-}py)_2[Ag(CN)_2)]_2$ compounds (X = H; 3-methyl; 4-methyl; 3,4-dimethyl; 3-Cl. The number indicates the substitution position in the pyridine. Convention: from now on, methyl = me). The influence on the SCO behaviour of the substitutions in the py ligand will be discussed and compared with the parent and halogen substituted compounds.

Results and Discussion

Magnetic properties:

The magnetic behaviour of the $Fe(X\text{-}py)_2[Ag(CN)_2]_2$ compounds, shown in Figure 1, depends significantly on the hydrogen substitution within the pyridine ligand. As previously reported,[19] for **X = H** the spin conversion occurs in two steps. At high temperature, the χT

product is equal to 3.66 $cm^3K \cdot mol^{-1}$ in agreement with the expected values for the HS state of a Fe^{2+} ion. As the temperature decreases, χT is constant until 190 K, and then undergoes a large decrease down to 2.25 $cm^3 \cdot K \cdot mol^{-1}$ at 140 K (step 1). Between 140 K and 110 K, χT defines a small plateau and finally below 110 K, it falls, reaching a value which depends on the cooling rate (step 2) since a trapping of HS species at low temperature occurs.[19] For a slow cooling rate (0.35 K min^{-1}) χT is 0.75 $cm^3 \cdot K \cdot mol^{-1}$ at 60 K. This value corresponds to a residual fraction of around 23 % of HS species which undergo the zero-field splitting, and therefore a decrease of the magnetic moment at low temperature is observed. The subsequent heating measurement (1 $K \cdot min^{-1}$) shows thermal hysteresis for step 2. Transition temperatures for both steps are $T_{1/2,1}$ = 146 K for the high temperature step and $T_{1/2,2\uparrow}$ = 98 K (on heating) for the low temperature step. For this second step, the transition temperature on cooling depends on the cooling rate, being $T_{1/2,2\downarrow}$ = 84 K at 0.35 $K \cdot min^{-1}$. For this low scan rate the spin conversion at steps 1 and 2 corresponds to 45 % and 32 % of the Fe(II) centers respectively. However, a rapid cooling of the sample from 250 K induces a considerable trapping of a HS metastable state at low temperature. The maximum amount of trapped species obtained by the fastest cooling rate reached by the instrument (10 K min^{-1}) is equal to the species involved in the second step. The halogen substituted compound X = 3-F shows a similar two step process regarding the transition temperatures, but without hysteresis.[20]

When a methyl group substitutes a hydrogen atom on the pyridine ligand, a drastic change in the magnetic behaviour is produced. Depending on the position of the substituted hydrogen, the spin conversion can be completely suppressed, as for **X = 3-me**, which remains in the HS state in the whole temperature range. However, it should be noticed that a small anomaly appears at ~75 K which can be symptomatic of an incomplete SCO. The same behaviour has been reported for the halogen substituted compounds X = 3-Br and X = 3-I, that also maintain the HS state.[20]

In contrast, when the methylation takes place in the 4 position, **X = 4-me**, the LS state seems to be favoured since the compound undergoes a gradual spin conversion, centred at about 175 K, in a broad temperature range of more than 150 K. In this last case, a residual paramagnetism, $\chi T \approx 0.5$ $cm^3K \cdot mol^{-1}$, is observed below 90 K.

However, the substitution of two hydrogen atoms by methyl groups (**X= 3, 4-dime**) leads to the recovering of a clear two-step behaviour and also a small decrease in average of the transition temperatures. In this case, the high temperature value of the χT product is equal to 4.20 $cm^3 \cdot K \cdot mol^{-1}$ as for X = 3-me. At 200 K, the spin transition starts, covering a temperature range of around 90 K, with a plateau at around 160 K. This transition is remarkably more abrupt than in the case of X = H, but the process does not show any thermal hysteresis. The transition temperatures are $T_{1/2,1}$ = 171 K and $T_{1/2,2}$ = 145 K for the high and low temperature step respectively. Around 47 % of the spin conversion is produced in step 1, and 53 % in the step 2. The residual paramagnetism at low temperature is in this case lower than for X = 4-me, with a value of around 0.2 $cm^3 \cdot K \cdot mol^{-1}$ indicating the practical absence of residual fraction of HS species, as confirmed by Mössbauer results (see below).

For **X = 3-Cl** an incomplete spin transition is detected in agreement with the work performed by the group of J.A. Real.[20] The value of the χT product decreases very slowly from 3.3 cm^3 K mol^{-1} at high temperature to 3.05 cm^3 K mol^{-1} at 140 K, where a gradual spin transition starts. At 60 K, a value of 1.9 cm^3 K mol^{-1} is reached, corresponding to ca. 40% of spin conversion. The decrease of the magnetic moment at low temperature can be attributed to the zero-field splitting of the residual fraction of around 60% of HS species. The transition temperature $T_{1/2}$ = 109 K is lightly higher than the previously reported value (106 K) and the

transition is our compound is less abrupt. These differences can be related with the quality and size of the crystals.

Considering the electronic effect due to the substitution within the ligand, it is expected that a decrease in the ligand field and in the $T_{1/2}$ value should be induced as the electronegativity of the ligand increases. [22,23] For the halogen substituted compounds, however, the opposite tendency is observed, as the HS state is stabilized as the size of the halogen atom increases.[20] The more efficient attenuation of the internal pressure coming from the lattice (and therefore of the ligand field strength felt by the Fe(II) ions) when highly polarizable atoms are present in the crystal is invoked as a possible explanation for the trend of $T_{1/2}$ in this halogen substituted compounds. If we compare the compounds X = 3-Cl and X = 3-me of our series, taking into account the fact that the electronegativity of the methyl group is much lower than that of Cl, the same trend as in the series of halogen substituted compounds seems to be present. However, when comparing X = 3-Cl and X = 4-me, the contrary is observed. The lack of precise structural information on our series prevents us from the type of explanation cited for the halogen substituted compounds, but it seems that the position of the substituent must play an important role inducing perhaps steric effect and inter ligand interactions which produce completely different magnetic behaviours.

^{57}Fe Mössbauer spectroscopy

The Mössbauer spectra recorded for all the compounds are shown in Figure 2. The parameters coming from the fits and the calculated HS and LS fractions are listed in Table 1.

In accordance with the magnetic susceptibility, the Mössbauer spectra reveal that the **X = 3-me** compound (Figure 2(a)) remains in the HS state at both temperatures. The Mössbauer results of **X = H**, reported previously, are also in agreement with the magnetic data[19] and the spectra do not show any evidence of the existence of two different Fe(II) sites that could be at the origin of the two-step behaviour.

The study of the **X = 4-me** compound has been done at different temperatures between 290 and 77 K (Figure 2(b)). The spectra were analysed with a doublet for the HS site and a singlet for the LS site. At temperatures where HS and LS species coexist, the fit has been done considering the same width, σ_{exp}, for both lines of the HS doublet, while at high temperature, a different σ_{exp} is considered for each line. Isomer shifts (IS) were given relative to α-Fe at room temperature. The data of the HS fraction were obtained assuming identical Mössbauer-Lamb factors for HS and LS states. At room temperature, the system is in the HS state. On lowering the temperature, a coexistence of HS and LS species is observed, with a continuous decrease of the HS ones. Finally, for $T < 90$ K, all the Fe(II) centres are in the LS state, with no evidence of paramagnetic residues. The residual paramagnetism at low temperatures shown by the magnetic measurements could be explained by slight differences in the synthesis of different samples.

In the case of **X = 3,4-dime** (Figure 2(c)) the data indicate a 100% HS species at room temperature and 100% LS species at 77 K, as it is expected, in accordance with the magnetic data where only a small paramagnetic contribution still exist at low temperature. Finally, for **X = 3-Cl**, (Figure 2(d)) a decrease of the HS fraction, from 100 % at 290 K to 53.5 % at 78 K, has been determined, also in agreement with the magnetic measurements.

Heat capacity

The heat capacity data are shown in Figure 3. The heat capacity measurements of **X = 3-me**, not shown in the figure, do not present any anomaly in the whole temperature range in accordance with its permanent HS state. For the other compounds, in order to evaluate the enthalpy (ΔH) and entropy (ΔS) variations, a non-anomalous contribution has been estimated using a smooth function interpolated from the heat capacity values out of the spin transition and finally subtracted. For **X = 4-me**, the data show two overlapped peaks with their maxima at T_{c1} =189 K and T_{c2} = 147.5 K. Although in absence of precise structural information we cannot discard other origin for the high temperature peak, such as methyl group rotation, most probably the calorimetric measurements - in contrast with other characterization techniques - are revealing a two-step spin transition, also observed in X = H and X = 3, 4-dime compounds (see below). The overall ΔH and ΔS are 10.8 kJ·mol^{-1} and 64.7 J·mol^{-1}K^{-1} respectively, and the values are within the experimental range generally observed for Fe(II) SCO compounds.[24] In order to estimate from these overlapped peaks the enthalpy and entropy contents associated to each step, the anomalous heat capacity has been fitted to the sum of two lorentzian functions. Hence, the thermodynamic quantities associated to each step are ΔH_1 = 5.5 kJ·mol^{-1}, ΔS_1 = 28.6 J·mol^{-1}K^{-1}; ΔH_2 = 5.3 kJ·mol^{-1}, ΔS_2 = 36.1 J·mol^{-1}K^{-1}.

Concerning the **X = 3,4-dime** compound, the heat capacity curve, obtained by DSC, also shows two asymmetrical and well separated anomalies associated to the two steps of the transition. The peak corresponding to step 1 is centred at T_{c1} =165 K and presents a shoulder on its high temperature side, while for step 2 a sharper peak is observed, with its maximum at T_{c2} = 142.5 K. The transition temperatures are slightly lower than the observed by magnetic susceptibility measurements. This difference is usually observed between magnetic and DSC results,[25] and can be attributed to the different scan rates in both techniques (0.5 K·min^{-1} on cooling in magnetic measurements and 10 K·min^{-1} in DSC). Considering the limit between the two steps at 150 K, the enthalpy and entropy values associated to each step are: ΔH_1 = 5.6 kJ·mol^{-1}, ΔS_1 = 32.2 J·mol^{-1}K^{-1}; ΔH_2 = 3.2 kJ·mol^{-1}, ΔS_2 = 25.5 J·mol^{-1}K^{-1}. A different change in entropy is observed between step 1 and step 2 in these two last compounds that, considering precedents in the literature,[7d] could be due to a different unit cell volume variation between the two steps. Unfortunately, single crystals could not be obtained from these compounds, and the structures could not be resolved from powder X-ray diffraction measurements, which makes unwise to do further conjectures about structural aspects.

The calorimetric measurements of the **X = 3-Cl** compound were performed by AC calorimetry, in order to have access to lower temperatures than with DSC (Figure 3(c)). The heat capacity curve shows a small and broad anomaly with its maximum around 120 K. The thermodynamic quantities associated to the transition are ΔH = 1.33 kJ·mol^{-1} and ΔS = 8.3 J·mol^{-1}K^{-1}, much lower than the observed for the other compounds of the family. However, in this case the spin transition is incomplete and, as it is shown in the inset of Figure 3(c), the compacting required to form a pellet for the AC measurements produces a reduction of the number of SCO centres that undergo the spin transition.[26] Taking into account this reduction the estimated enthalpy and entropy values would be $\Delta H \sim$ 2.5 kJ·mol^{-1} and $\Delta S \sim$ 15 J·mol^{-1}K^{-1} and finally, considering the incompleteness of the transition described in the magnetic measurements (40 % of spin conversion), $\Delta H \sim$ 6.25 kJ·mol^{-1} and $\Delta S \sim$ 37.55 J·mol^{-1}K^{-1} per mole which undergoes the spin crossover transition.

Finally, the thermodynamic study of the **X = H** compound was reported elsewhere, but the results are also shown in Figure 3 for comparison.[19] The enthalpy and entropy contents

associated to both steps of transition were ΔH_1 = 3.33 kJ·mol^{-1}, ΔS_1 = 22.6 J·mol^{-1}K^{-1}; ΔH_2 = 1.51 kJ·mol^{-1}, ΔS_2 = 15.7 J·mol^{-1}K^{-1}. The entropies contents are typical values for the SCO compounds.[24]

The consistency of the thermodynamic and magnetic data can be analysed using a simple model proposed by Real,[7d] based on the regular solution model from Slichter and Drickamer.[27] Additionally, this model gives information about the cooperativity of these compounds. The model considers two independent groups of SCO centres that undergo the spin transition at two different temperatures. The total high spin fraction can be written as:

$$\gamma_{HS} = (1-c)\,\gamma_{HS1} + c\,\gamma_{HS2} \quad (1)$$

where $\gamma_{HS1,2}$ are the high spin fractions for each step, both going from 0 to 1, and c is the value of γ_{HS} in the plateau. The cooperativeness is included by means of four phenomenological interaction constants introduced in the expression of the Gibbs free energy: Γ_{11}, Γ_{22}, for the interaction within the groups, and Γ_{12}, Γ_{21}, for the interaction between the two groups. The following system of coupled equations thus describes the two-step spin transition:

$$ln\left[\frac{1-\gamma_{HS1}}{\gamma_{HS1}}\right] = \frac{\left[\Delta H_1 + \Gamma_{11}(1-2\gamma_{HS1}) - 2\Gamma_{12}\gamma_{HS2} - T\Delta S_1\right]}{RT} \quad (2a)$$

$$ln\left[\frac{1-\gamma_{HS2}}{\gamma_{HS2}}\right] = \frac{\left[\Delta H_2 + \Gamma_{22}(1-2\gamma_{HS2}) - 2\Gamma_{21}(\gamma_{HS1}-1) - T\Delta S_2\right]}{RT} \quad (2b)$$

where $\Delta H_{1,2}$ and $\Delta S_{1,2}$ are respectively the enthalpy and entropy variations for the two groups, which are related to the experimental values by:

$$\Delta H_1(\gamma_{HS1} = 1/2;\ \gamma_{HS2} = 1) = \Delta H_1^{exp}/(1-c) \quad (3a)$$

$$\Delta H_2(\gamma_{HS1} = 0;\ \gamma_{HS2} = 1/2) = \Delta H_2^{exp}/c \quad (3b)$$

$$\Delta S_1 = \Delta S_1^{exp}/(1-c) \quad (4a)$$

$$\Delta S_2 = \Delta S_2^{exp}/c \quad (4b)$$

The numerical solution of this system of coupled equations has been done optimising Γ_{11} and Γ_{22}, and using the experimental values of $\Delta H_{1,2}$ and $\Delta S_{1,2}$ for each compound. The hypotesis of $\Gamma_{12} = \Gamma_{21}$ is considered, which allows reducing the number of parameters. The results for all the compounds which undergo the spin transition are presented in Figure 4, compared with the experimental high spin fraction obtained form the magnetic measurements.[28]

Despite its simplicity, the model allows to reproduce the main features of the spin transitions of this family of compounds. For **X = H**, a residual fraction, r_{HS} = 0.23, of SCO centres which remain in the HS state at low temperature has been additionally considered, and the experimental enthalpy and entropy contents of steps 1 and 2 have been considered to correspond to a 47 % and 30 % of spin conversion respectively, according to the magnetic measurements. The calculus is insensitive to the value of Γ_{12}, due to the considerable difference in the transition temperatures of the two steps.[7d] The interaction constant within the first group which gives the best accordance with the magnetic data is Γ_{11} = 1.9 kJ·mol^{-1}

and then, $\Gamma_{11}/2RT_{c1} = 0.78 < 1$, as expected for a continuous process (without hysteresis).[27] The best agreement with the experimental results has been obtained considering a lineal dependence with temperature of Γ_{22} as proposed by Purcell and Edwards.[29] The optimised value is $\Gamma_{22}(T) = 0.135 + 0.016T$ kJ·mol^{-1}, and then, $\Gamma_{22}(T_{c2})/2RT_{c2} = 1.05$, gives a hysteresis of 13 K, in accordance with the experimental data. Several factors can explain the discrepancy between the experimental and calculated curves especially in the hysteresis loop region. Firstly, the distribution of some of the parameters governing the SCO (energy barrier, and the metal-ligand bond length difference, Δr, between the two states, etc.).[12] On the other hand, the differences can also have a kinetic origin: due to the slow HS-LS relaxation, the cooling branch (where the bigger discrepancies are observed) is extended in a wider temperature range for increasing scan rates.[19]

The proposed model can also reproduce the magnetic behaviour of the **X = 4-me** compound. In this case, c has been considered to be equal to 0.5, in the absence of experimental evidences which would allow to establish its value more precisely, and $r_{HS} = 0$, in accordance with the Mössbauer results. The simulation is insensitive to Γ_{12}, and the optimised interaction constants are $\Gamma_{11} = 1.1$ kJ·mol^{-1}, $\Gamma_{22} = 0.5$ kJ·mol^{-1}, and thus, $\Gamma_{11}/2RT_{c1} = 0.35$, $\Gamma_{22}/2RT_{c2} = 0.21$. Both values are much lower than 1, and lie in the range of the lowest reported in the literature,[30] indicating a poorly cooperative behaviour.

The simulation for the **X = 3,4-dime** compound has been performed considering $r_{HS} = 0$ and $c = 0.53$, according to the magnetic susceptibility and Mössbauer data. The optimised interaction constants within the groups are $\Gamma_{11} = 2.3$ kJ·mol^{-1}, i.e., $\Gamma_{11}/2RT_{c1} = 0.84$, and $\Gamma_{22} = 2$ kJ·mol^{-1}, i.e., $\Gamma_{22}/2RT_{c2} = 0.84$. These values, near 1, explain the abruptness of both steps, although they are not large enough to produce hysteresis.

The gradual and incomplete spin transition of the **X = 3-Cl** compound can be analysed using the simple regular solution model,[27] considering $r_{HS} = 0.58$. The interaction constant which better reproduces the experimental results is $\Gamma = 1.0$ kJ·mol^{-1}, and then $\Gamma/2RT_c = 0.55$, corresponding to a low cooperativity system.

Optical properties

In order to have an indication about the possibility for this family to show photomagnetic properties, absorbance and reflectivity measurements have been performed. Concerning the study of absorbance versus wavelength at different temperatures, two main absorption bands are observed, at about 540 and 830 nm, respectively, for all the members of the family. These bands could be attributed to the $^1A_1 \rightarrow {}^1T_1$ and $^5T_2 \rightarrow {}^5E$ transitions.[31] The former grows along with the LS fraction, while the latter increases with the HS population. As an example of such kind of measurement, Figure 5(a) shows the obtained behaviour for X = 4-me compound.

The results of reflectivity as a function of temperature at $\lambda = 532$ nm for all the compounds are also shown in Figure 5. All members of this family (with one exception, i.e. X = 3-me which does not show SCO) present a very responsive behaviour to reflectivity technique, showing some common features. At high temperature, the thermal spin transition is observed, while in the low temperature region the measurements reveal a quantitative photo-induction describing a LITH (Light Induced Thermal Hysteresis) process.[32]

In particular, the temperature dependence of the reflected intensity at 532 nm for **X=H** is plotted for the cooling and heating modes in Figure 5(b). A two-steps thermal transition with hysteresis in step 2 is determined, in agreement with the magnetic data. Below 85 K the signal increases, meaning that a photo-induced process to convert LS to HS state is activated, and the LITH is observed. It should be noted that the relative amplitude of step 2 is smaller than in the magnetic curve. This is seemingly related, on the one hand, with the higher scan rate in the reflectivity measurements (~13 and ~10 K $\cdot$min^{-1} for cooling and heating respectively in the 50-150 K temperature range), which causes a significant trapping of the SCO centres in HS due to the rapid cooling. On the other hand, the continuous irradiation in this temperature range favours the HS state and therefore goes in the same direction.

The spectra of **X=3-me** are qualitatively similar to the one shown in Figure 5(a), although the absorbance of the sample is globally smaller. Notwithstanding, a not negligible effect in the range 75-100 K is noticed when we plot the intensity of the band centred at 532 nm as function of the temperature (Figure 5(c)).

In the dimethylated complex (**X=3,4-dime**), two abrupt thermal transition steps are clearly evident (Figure 5(c)), in agreement with the magnetic and calorimetric data. In contrast, the reflectivity curve in the thermal transition range for **X=4-me** (Figure 5(d)) is analogue to the magnetic susceptibility one and the presence of a two-step SCO is not evident. In the low temperature region, we observe the photoinduction of the HS state, with LITH effect, starting below 60 K for this last compound and below 75 K for the former one.

Finally, the reflectivity at λ = 532 nm of **X=3-Cl** (Figure 5(d)) shows, accordingly with the magnetic data, a gradual and incomplete HS to LS transition between 200 K and 80 K. Below this temperature, the irradiation produces almost complete return to the HS state and, as in the previous compounds, the LITH effect is observed.

LIESST effect

The photo-magnetic properties of the compounds of the family that present a thermal spin transition were investigated following the *T*(LIESST) procedure.[4] Briefly, the sample is irradiated for a variable duration of time (of the order of 1-2 hours) with laser light at 530.9 nm. Once the photostationary point was reached, the light was switched off and the susceptibility measured as a function of the temperature on heating from 10 K to 300 K. The *T*(LIESST) value has been established at the point of maximum slope of the LIESST curve.

The photomagnetic curves shown in Figure 6 prove that under a suitable irradiation a quantitative photo-conversion of the LS to the metastable HS form of the complexes is reached in all the cases. It is noteworthy that the photoinduced HS fraction strongly depends on the intensity of the light. Moreover, in the cases where a two-step SCO occurs, a threshold effect between a 50 % and a complete photoexcitation is observed. That is, when the power is around 2 mW$\cdot$cm^{-2}, whatever is the irradiation time, a limit of *ca.* 50 % of photoexcitation is obtained, while higher intensities allow to overcome this value. Table 2 summarises the *T*(LIESST) and $T_{1/2}$ values for all the compounds. In the cases of **X = H** and **3,4-dime**, the derivative of the LIESST curve shows two minima in correlation with the two-step behaviour observed in the thermal spin transition. For **X = 4-me**, however, the existence of a small anomaly at around 50 K on *T*(LIESST) curve corresponds to a remaining oxygen contamination even if particular precaution has been taken to purge the SQUID cavity.

Relaxation of the light-induced HS state and fitting procedure.

The relaxation kinetics of the photoexcited HS state recorded at different temperatures for the four SCO compounds are shown in Figure 7. The experimental procedure consists on irradiating the sample at 10 K in the SQUID cavity in order to photoexcite the HS state and heating the sample under continuous irradiation up to the temperature at which the relaxation has to be recorded. Once this temperature is reached and stabilised, the light is turned off and the susceptibility measured as a function of time. From these experiments, one can extract the thermodynamic parameters of the HS-LS conversion process[33] which in turn allow to simulate the LIESST curve.[4]

In some cases in which the thermal spin transition and the LIESST curve show two steps, the relaxation of the light-induced HS state also reflects this behaviour, but few examples – apart from the binuclear compounds – have been reported in the literature.[7d,34,35] As in the previously reported compound [Fe(DPEA)(bim)]$(ClO_4)_2$·0.5 H_2O,[34] in some of the present cases, a best fit of the relaxation curves was obtained by using a double exponential relaxation, instead of the classical single exponential (low cooperativity) or sigmoidal (high cooperativity) decays. Equation (5) describes this double exponential relaxation.

$$\gamma_{HS} = c_1 \exp[-k_{HL1} \cdot t] + c_2 \exp[-k_{HL2} \cdot t] \quad (5)$$

where c_i (i = 1,2) are the fractions of SCO centres involved in each step (these parameters are fixed in the fit according to the magnetic data), and $k_{HLi}(T)$ are the respective relaxation process constants. The single stretched exponential decay described by Equation (6) has been used in the other cases. This dependence entails a distribution of the value of the relaxation constant, k_{HL}, around an average value; β (ranging between 0 and 1) is related to the width of this distribution.[36] The differences between fits using the stretched exponential law and the double exponential law can be appreciated in Figure 7(e).

$$\gamma_{HS} = \exp[-(k_{HL}t)^{\beta}] \quad (6)$$

The latter equation resulted to be the best suited one to fit the decays in the tunnelling regime.

Since k_{HL}, can be expressed as:[33]

$$k_{HL}(T) = k_{HL(T \to 0)} + k_{HL(T \to \infty)} \cdot \exp(-E_a/k_B T) \quad (7)$$

The linear fit of the Arrhenius plot ($\ln[k_{HL}]$ *vs.* $1/T$) in the thermally activated region allows a calculation of the activation energy, E_a, and the pre-exponential factor $k_{HL(T \to \infty)}$ for each compound. To a first approximation, for the values of $k_{HL(T \to 0)}$ we consider the relaxation constant corresponding to the lower temperature relaxation among the ones that reach a complete conversion. This may be taken as an upper limit of the $k_{HL(T \to 0)}$ value.[4] The parameters coming from the fits for all the compounds, together with the E_a and $k_{HL(T \to \infty)}$ values deduced from the Arrhenius plots (Figure 7(f)), are listed in Table 3. These thermodynamic parameters are of the order of the observed in other spin-crossover compounds[33] and, in the cases where a double exponential describes the relaxation (X= H; 3,4-dime) similar to the reported for other polymeric compounds with two-step transitions.[7d]

The relaxation at 30 K for **X=H** (Figure 7(a)), corresponds to a process occurring in the tunnelling regime: in about 13 hours, only the ~ 8 % of the light-induced HS fraction has relaxed. On the contrary, the relaxations at 49 and 55 K are almost complete by the same time

interval. Although the two-step process is not evident from the relaxation curves, the $d\gamma_{HS}/dt$ *vs.* γ_{HS} representation (inset graph in Figure 7(a)) reveals the existence of two relaxation constants. Accordingly, the best fits of both curves are obtained with Equation (5). The thermodynamic parameters have been deduced separately for each transition step (Table 3). The behaviour of **X = 3,4-dime** is similar to the observed in compound X = H. Even though, taking into account the hysteresis of the low temperature step, the compound X = H can be considered a cooperative system, stretched exponential shapes of the relaxation curves are observed instead of the expected sigmoidal shape. The stretched exponential shapes are typical for a broad distribution of relaxation times, which are expected to be associated with structural disorders,[37] as the observed in this compound.[19]

In the case of the other two compounds that show spin transition, the phenomenon is better described with a stretched exponential equation. For **X = 4-me**, also the relaxations out of the tunnelling regime are hence best fitted with Equation (6). The two-step process is not evident, as in the magnetic curve of the thermal spin transition. However, the low values of β (0.4 – 0.5) are compatible with the existence of strongly overlapped bimodal distribution of relaxation constants. Also for **X = 3 –Cl**, the relaxation curves have been fitted to stretched exponential decays, as expected for a single relaxation process. Differently from the other complexes, at 50 K the relaxation affects only to a 3 % of the SCO centres after more than 4 hours, and complete relaxation is recorded only at 70 K . This makes imprecise the estimation of E_a and $k_{HL(T\rightarrow\infty)}$.

The simulation of the LIESST curves using the thermodynamic parameters, as proposed by Létard,[4] has been performed in order to check the overall consistency of the photomagnetic data. The procedure has been adapted for two-step processes, for which the LIESST curve is fitted using the following equations:

$$\left(\frac{\partial\gamma_{AS,i}}{\partial t}\right)_T = -\gamma_{AS,i}\left\{k_{AB,i(T\rightarrow 0)} + k_{AB,i(T\rightarrow\infty)}\, exp\left[-E_{a,i}/k_B T\right]\right\} (i = 1, 2) \quad (8.a)$$

$$\gamma_{AS} = c_1\gamma_{AS,1} + c_2\gamma_{AS,2} \quad (8.b)$$

The calculation has been performed considering that the temperature of a given experimental point governs the relaxation in the time interval between that experimental point and the next one.

The calculated curves are shown as the solid lines in Figure 6, and the fitting parameters, E_a and $k_{HL(T\rightarrow\infty)}$, are listed in Table 4 and represented in Figure 7(e). In all cases the shape and position of the curves is well described, with fitting parameters close to the values obtained from the Arrhenius plots. The differences between the calculated and the experimental curves can be better appreciated in the representation of the derivatives. In **X = 3-Cl**, only the *T*(LIESST) is well reproduced and not the shape of the derivative, probably due to the lack of precision in the determination of the thermodynamic parameters with only two relaxation curves and, as in **X = 4-me**, to the existence of a small anomaly at around 50 K corresponding to oxygen contamination. On the other hand, in the case of **X = H**, the agreement is quite satisfactory. For **X = 3,4-dime**, the two *T*(LIESST) are less evident, probably due to the proximity of the two values.

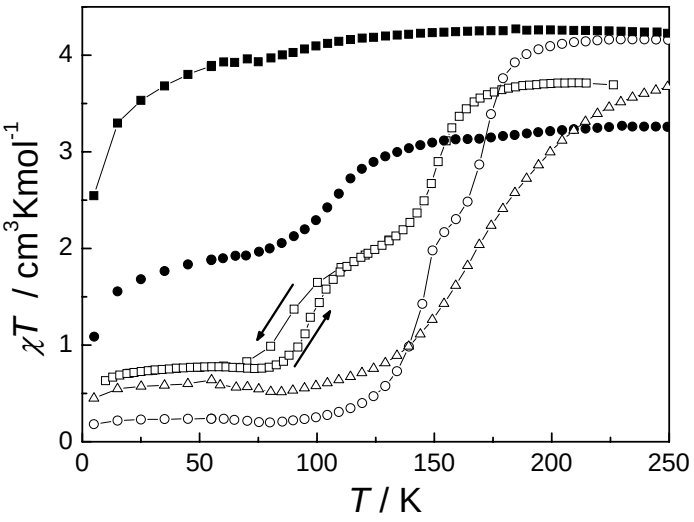

Figure 1: Temperature dependence (on cooling, except for X = H for which heating and cooling curves are displayed) of the χT product for the investigated complexes $Fe(X\text{-}py)_2[Ag(CN)_2)]_2$: (□) X = H; (●) X = 3-Cl; (■) X = 3-me; (Δ) X = 4-me; (○) X = 3,4-dime.

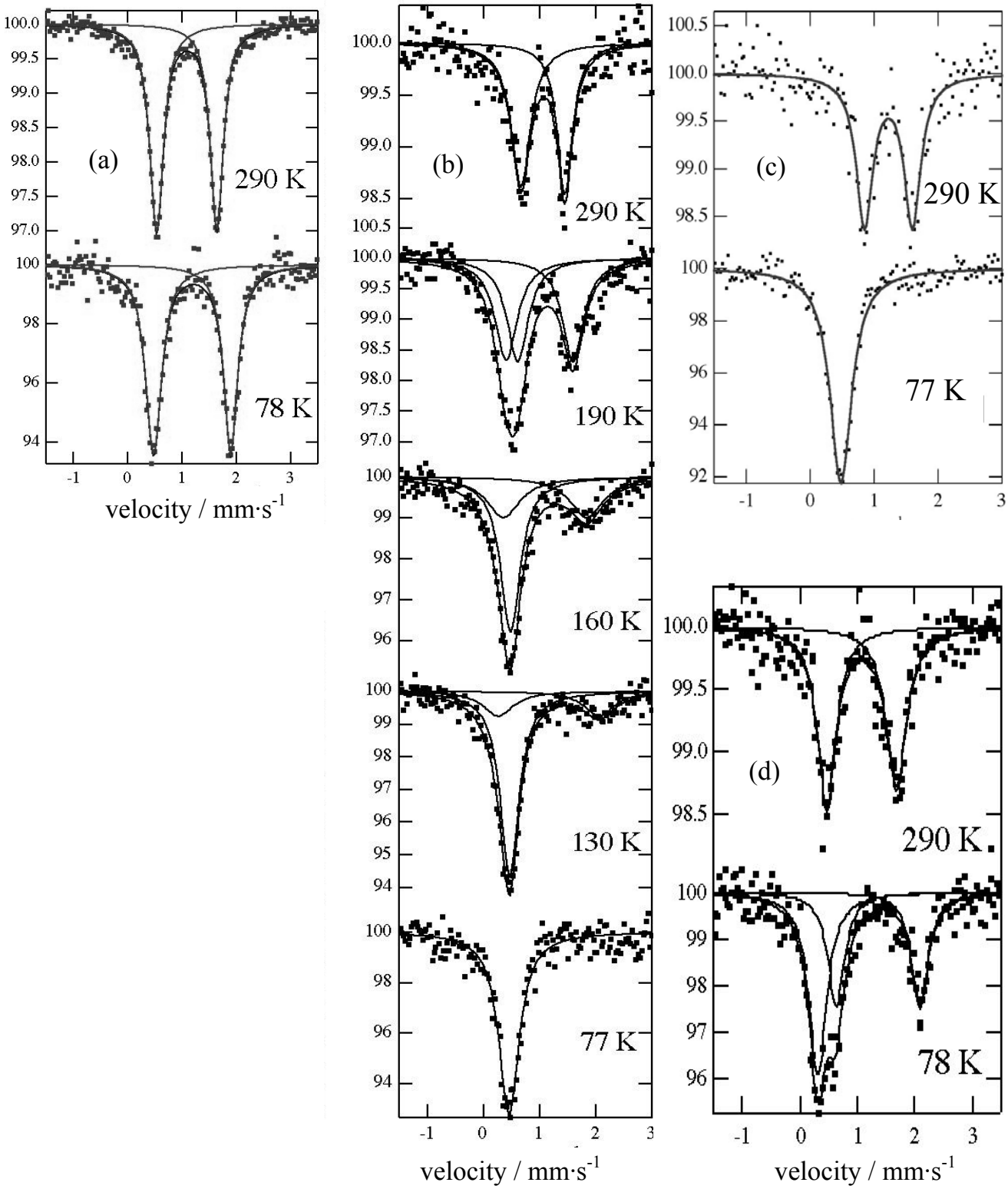

Figure 2: Selected Mössbauer spectra of (a) X = 3-me, (b) X = 4-me, (c) X = 3,4-dime. (d) X = 3-Cl. Vertical axis: relative intensity (%).

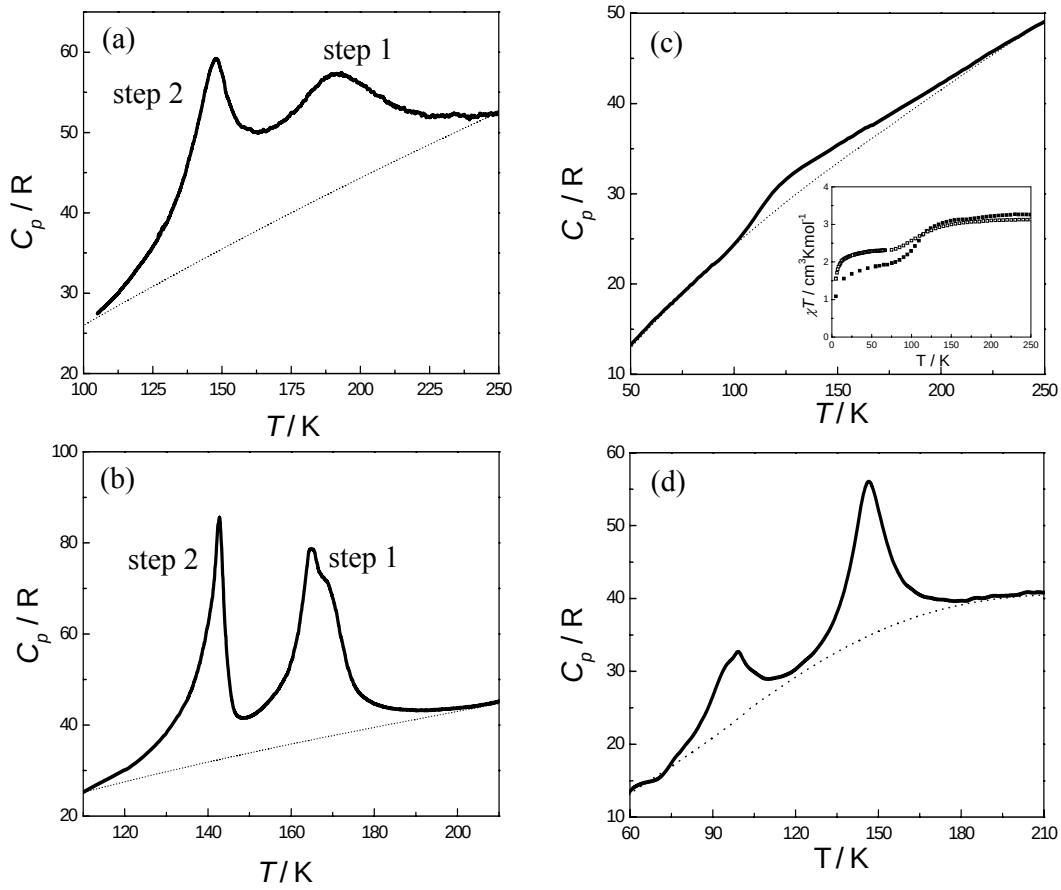

Figure 3: Heat capacity results for the complexes of the family $Fe(X\text{-}py)_2[Ag(CN)_2)]_2$: The estimated non-anomalous contribution is represented as a dotted line for each compound. (a) X = 4-me (DSC) (b) X = 3,4-dime (DSC) (c) X = 3-Cl (AC calorimetry). Inset: Magnetic behaviour of a pellet sample (□) compared with a powder one (■). (d) X = H (Adiabatic calorimetry) (taken from ref [19]).

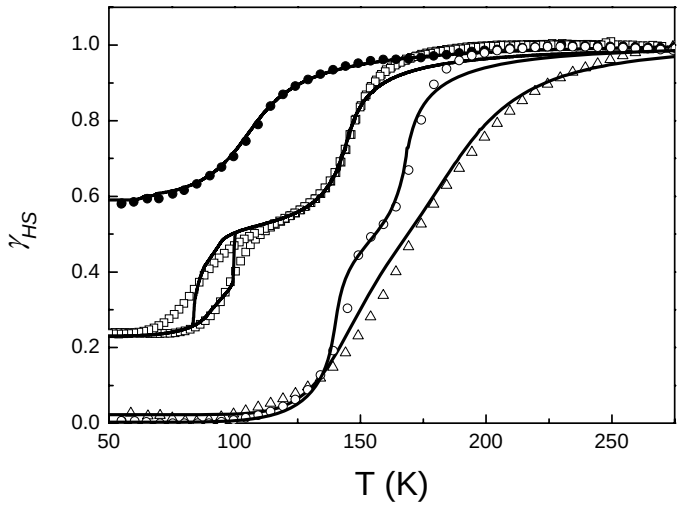

Figure 4: Temperature dependence of γ_{HS} deduced from the magnetic susceptibility measurements for the complexes $Fe(X\text{-}py)_2[Ag(CN)_2)]_2$: (□) X = H; (●) X = 3-Cl; (Δ) X = 4-me; (○) X = 3,4-dime, and simulation (continuous lines) as described in the text.

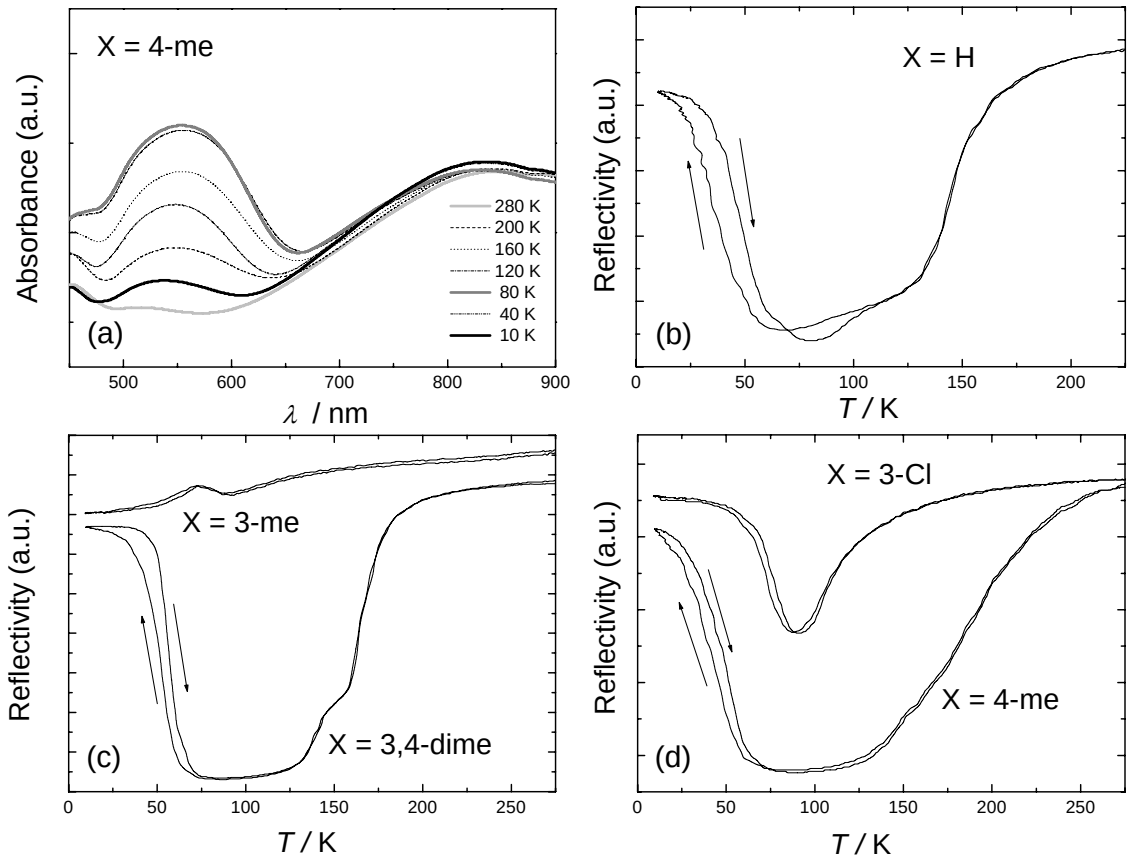

Figure 5: Reflectivity measurements of the $Fe(X\text{-}py)_2[Ag(CN)_2)]_2$ family: (a) Absorbance spectra of X = 4-me at different temperatures. (b, c, d) Reflectivity as a function of temperature at 532 ± 2.5 nm for all the compounds investigated.

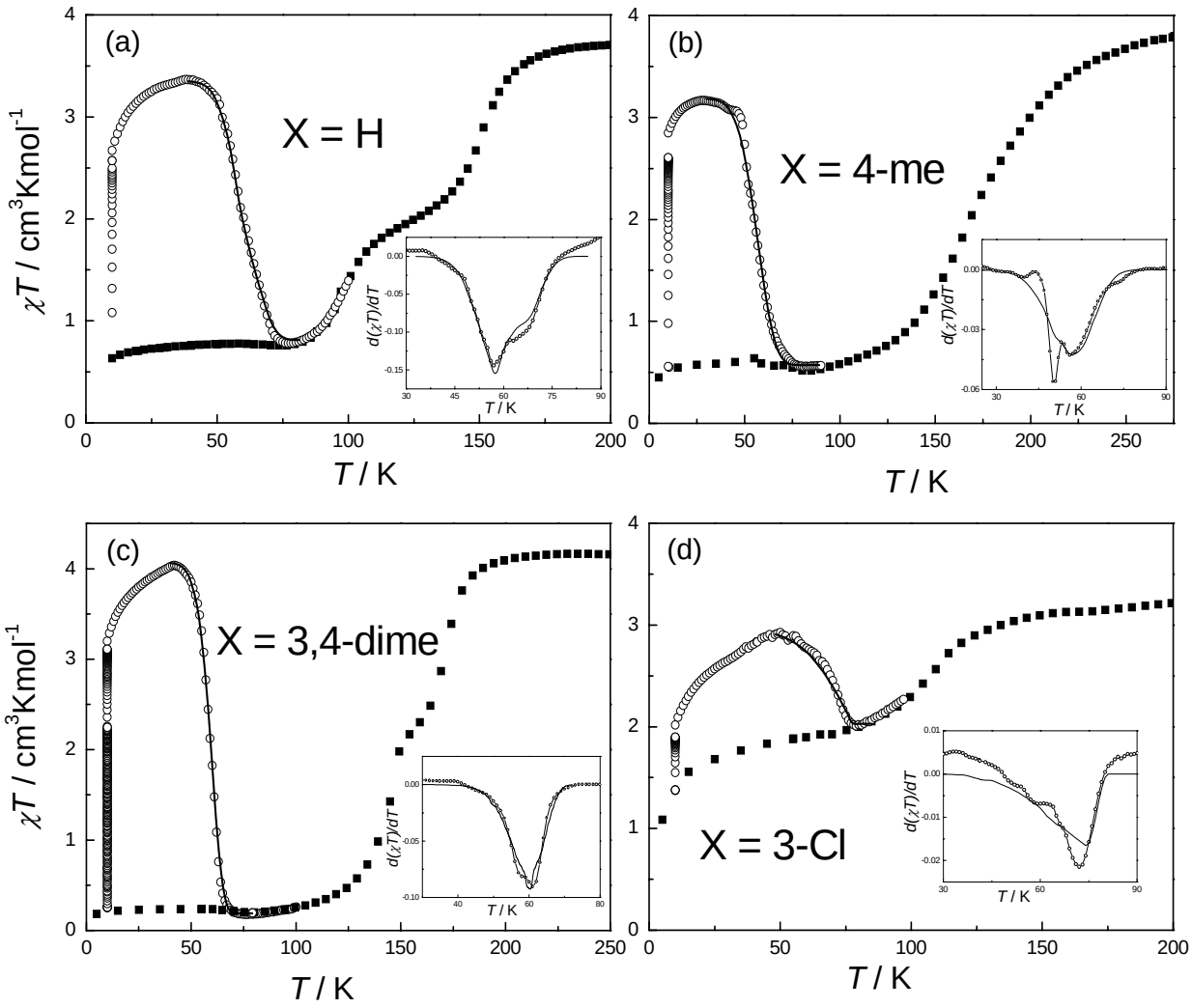

Figure 6: Temperature dependence of the χT product for the family $Fe(X\text{-}py)_2[Ag(CN)_2)]_2$: (a) X = H; (b) X = 4-me; (c) X = 3,4-dime; (d) X = 3-Cl. (■) Data recorded without irradiation; (○) Irradiation at 10 K and T(LIESST) measurement. The inset graphs show the derivatives, $d(\chi T)/dT$, of the LIESST curves as a function of the temperature. The solid lines represent the simulation of the LIESST curve.

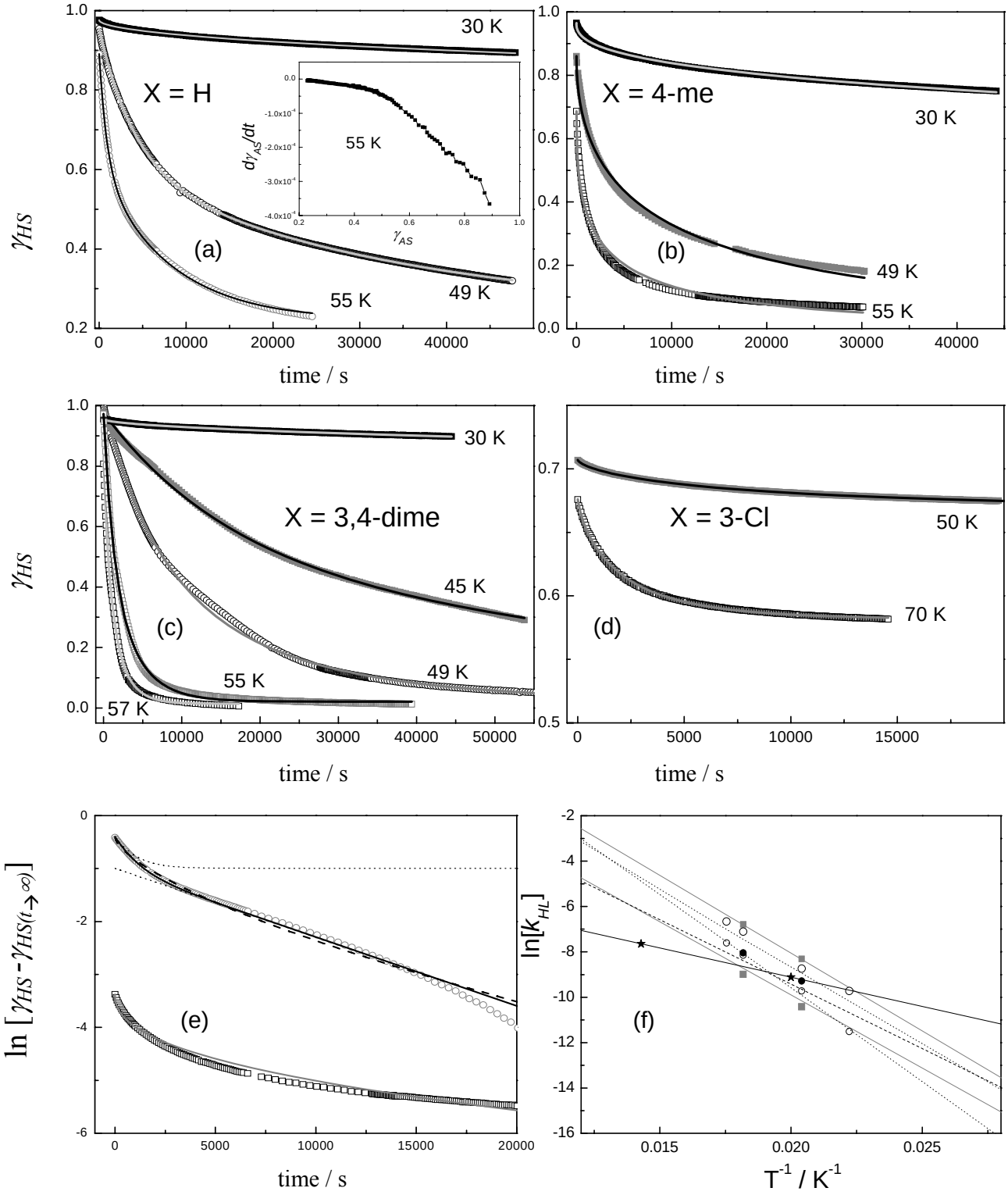

Figure 7: Time dependence of the γ_{HS} fraction (symbols) and fits (continuous lines) at different temperatures for the family $Fe(X\text{-}py)_2[Ag(CN)_2)]_2$: (a) X = H; (b) X = 4-me; (c) X = 3,4-dime; (d) X = 3-Cl. The inset in (a) shows the $d\gamma_{HS}/dt$ vs. t representation for the relaxation at 55 K. (e) Logarithmic plot of two selected relaxation curves: X = H at 55 K (○), stretched exponential fit (dashed line), double exponential fit (continuous line) and the two exponentials of this last one shown independently (dotted lines); X = 4-me at 55 K (□, shifted for clarity) and stretched exponential fit (continuous gray line) (f) Arrhenius plot of the k_{HL} constants obtained from the fits of the relaxation curves (symbols) and parameters of the fitting of the LIESST curves (lines): X = H (■ and grey solid lines); X = 4-me (● and black dashed line); X = 3,4-dime (○ and black dotted lines); X = 3-Cl (★ and black solid line).

Table 1: Mössbauer parameters (I.S.: isomer shift; Q.S.; quadrupole splitting; σ_{exp}: peak width) and area fractions of the characteristic subspectra corresponding to HS state for the investigated complexes Fe(X-py)$_2$[Ag(CN)$_2$)]$_2$ at selected temperatures.

X	*T* (K)	site	I.S. (mm s^{-1})	Q.S. (mm s^{-1})	σ_{exp} (mm s^{-1})	Area fraction (%)
3-me	290	HS	1.09	1.10	0.30/0.29	100
	78	HS	1.19	1.42	0.35/0.32	100
4-me	290	HS	1.06	0.78	0.41/0.33	100
	190	HS	1.10	0.99	0.46	65.9
		LS	0.41		0.49	34.1
	160	HS	1.10	1.48	0.73	47.1
		LS	0.48		0.42	52.9
	130	HS	1.16	1.80	0.65	30.1
		LS	0.47		0.40	69.9
	77	LS	0.46		0.44	0
3-Cl	290	HS	1.07	1.21	0.39/0.43	100
	78	HS	1.36	1.45	0.35	53.5 (30)
		LS	0.31		0.38	46.5 (30)
3,4-dime	290	HS	1.23	0.75	0.32/0.32	100
	77	LS	0.64		0.41	100

Table 2: Spin Transition and LIESST temperatures of the Fe(X-py)$_2$[Ag(CN)$_2$)]$_2$ compounds.

X	*T*(LIESST) [K]	$T_{1/2}$ [K]
H	58/65	98/146
3-me	HS	
4-me	56	~150/ ~190
3,4-dime	58/61	145/171
3-Cl	72	109

Table 3: Thermodynamic parameters for relaxation from the LIESST state.

X	T (K)	k_{HL} (s^{-1})	c_i	β	E_a (cm^{-1})	$k_{HL(T\to\infty)}$ (s^{-1})
H	30	3.2×10^{-7}	--	0.7	$E_{a1} = 476$ $E_{a2} = 448$	$k_{HL1(T\to\infty)} = 290$ $k_{HL2(T\to\infty)} = 15$
	49	$k_{HL1} = 3.0 \times 10^{-5}$ $k_{HL2} = 2.5 \times 10^{-4}$	$c_1 = 0.43$ $c_2 = 0.32$ $r_{HS} = 0.23$	--		
	55	$k_{HL1} = 1.3 \times 10^{-4}$ $k_{HL2} = 1.1 \times 10^{-3}$		--		
4-me	30	7.9×10^{-7}	--	0.5	383	7
	49	9.3×10^{-5}		0.44		
	55	3.2×10^{-4}		0.42		
3,4-dime	30	1.45×10^{-7}	--	0.55	$E_{a1} = 461$ $E_{a2} = 566$	$k_{HL1(T\to\infty)} = 140$ $k_{HL2(T\to\infty)} = 891$
	45	$k_{HL1} = 1.0 \times 10^{-5}$ $k_{HL2} = 6.0 \times 10^{-5}$	$c_1 = 0.47$ $c_2 = 0.53$	--		
	49	$k_{HL1} = 6.0 \times 10^{-5}$ $k_{HL2} = 1.6 \times 10^{-4}$				
	55	$k_{HL1} = 2.9 \times 10^{-4}$ $k_{HL2} = 8.2 \times 10^{-4}$				
	57	$k_{HL1} = 5.0 \times 10^{-4}$ $k_{HL2} = 1.3 \times 10^{-3}$				
3-Cl	50	1.1×10^{-4}	--	0.7	~178	~0.02
	70	4.8×10^{-4}		0.7		

Table 4: Parameters of the fitting of the LIESST curves.

X	E_a (cm^{-1})	$k_{HL(T\to\infty)}$ (s^{-1})
H	$E_{a1} = 477$ $E_{a2} = 448$	$k_{HL1(T\to\infty)} = 290$ $k_{HL2(T\to\infty)} = 20$
4-me	395	7
3,4-dime	$E_{a1} = 451$ $E_{a2} = 530$	$k_{HL1(T\to\infty)} = 190$ $k_{HL2(T\to\infty)} = 900$
3-Cl	178	0.02

Conclusions

The present work enlarges the series of the rare examples of SCO compounds – apart from the binuclear ones – where a two-step behavior is shown not only in the thermal spin transition, but also in the relaxation of the photoinduced HS metastable state. We have investigated, by means of magnetic, photomagnetic, calorimetric, Mössbauer and reflectivity measurements, the thermal SCO phenomenon in a new series of 2D coordination polymers with general formula $Fe(X\text{-}py)_2[Ag(CN)_2]_2$ (py = pyridine, X = 3-Cl; 3-methyl; 4-methyl; 3,4-dimethyl) and their light-induced properties together with the parent compound $Fe(py)_2[Ag(CN)_2]_2$. Most of the compounds of the family (X = H; 4-me; 3,4-dime) undergo an almost complete two-step spin transition, while for X = 3-Cl the transition is incomplete, and for X = 3-me the system remains in the HS state in the whole temperature range. The influence of the substitutions in the pyridine ligand has been found to be the opposite to the expected from only electronic considerations, and the crystal packing is believed to be the main responsible for this behaviour. The thermodynamic parameters associated with the spin transition have been obtained from the heat capacity measurements and the consistency of the thermodynamic and magnetic data analysed using a simple model proposed by Real and coworkers based on the regular solution model from Slichter and Drickamer, which gives also information about the cooperativity of these compounds.

As for the photomagnetic phenomenon, except for X = 3-me, all the studied systems show a quantitative LIESST. All these compounds exhibit stretched exponential decays of the light-induced state, which is symptomatic of a low cooperative process. The thermodynamic parameters obtained from the analysis of the relaxation curves have been used to calculate the LIESST curves, allowing to check the consistency of the photomagnetic study. The compounds that present a two-step thermal spin transition interestingly reveal a two-step character also in the relaxation of the photoinduced HS metastable state, which is a quite uncommon feature for this type of systems.

Experimental Section

Synthesis: The $Fe(X\text{-}py)_2[Ag(CN)_2]_2$ family was prepared following the method applied for $Cd(py)_2[Ag(CN)_2]_2$[38] and $Fe(py)_2[Ag(CN)_2]_2$,[19] but using the corresponding substituted ligand instead of pyridine. Anal. calcd for $Fe(3\text{-}Clpy)_2[Ag(CN)_2]_2$, $FeC_{14}H_8N_6Cl_2Ag_2$: C 27.90, H 1.33, N 13.95; found: C 27.11, H 1.27, N 13.11. Anal. calcd for $Fe(4\text{-}mepy)_2[Ag(CN)_2]_2$, $FeC_{16}H_{14}N_6Ag_2$: C 34.20, H 2.49, N 14.96; found: C 34.60, H 2.61, N 14.24. Anal. calcd for $Fe(3\text{-}mepy)_2[Ag(CN)_2]_2$, $FeC_{16}H_{14}N_6Ag_2$: C 34.20, H 2.49, N 14.96; found: C 34.39, H 2.52, N 14.96. Anal. calcd for $Fe(3,4\text{-}dimepy)_2[Ag(CN)_2]_2$, $FeC_{18}H_{18}N_6Ag_2$: C 36.65, H 3.05, N 14.25; found: C 37.20, H 2.93, N 13.93.

Reflectivity: The reflectivity of the samples was measured with a home-made set-up equipped with a CVI spectrometer. This system allows the collection of both the reflectivity spectra within the range of 450–950 nm at a constant temperature and to follow the temperature dependence of the signal between 5 K and 290 K at a selected wavelength (± 2.5 nm). The sample was a thin layer of the powdered compound without any dispersion in a matrix.[39]

Magnetic susceptibility and photo-magnetic measurements: The magnetization vs. temperature measurements were performed on a MPMS-XL Quantum Design SQUID magnetometer between 5 K and 300 K in an external field of 1 Tesla. A sample mass of ~15 mg has been used. The data were corrected for the magnetisation of the sample holder and for diamagnetic contributions, estimated from Pascal's constants.
The photo-magnetic measurements were performed with a Spectra Physics Series 2025 Kr^+ laser (λ = 530.9 nm) coupled by an optical fibre to the cavity of the SQUID magnetometer (MPMS-55 Quantum Design SQUID) operating with an external magnetic field of 2 T. The temperature range was 2–300 K and the scan rate 0.3 $K \cdot min^{-1}$. The power at the sample was adjusted to 5 $mWcm^{-2}$. Bulk attenuation of light intensity was limited as much as possible by the preparation of a thin layer of compound. It is noteworthy that there was no change in the data due to sample heating upon laser irradiation.
The weight of these thin layer samples (approximately 0.2 mg) was estimated by the comparison of their thermal spin-crossover curves with the experimental magnetic data obtained with a more accurately weighted sample of the same compound.

Mössbauer spectroscopy: ^{57}Fe Mössbauer experiments were carried out on cooling from 290 K to 78 K on a Wissel Mössbauer spectrometer consisting on a MDU-1200 driving unit and a MVT-100 velocity transducer, incorporating a Seiko Model 7800 multi-channel analyzer. The powder samples (~ 60 mg) were kept in a Heli-Tan LT-3 gas-flow cryostat (Advanced Research System Inc.) equipped with a 9620 digital temperature controller from Scientific Instruments. The ^{57}Co(Rh) source was maintained at room temperature.

Calorimetric measurements: Heat capacity measurements have been performed in the 100-300 K temperature range with a differential scanning calorimeter (Q1000 model from TA Instruments) at a heating rate of 10 K/min. Calibration in temperature and energy was performed using a standard sample of indium using its melting transition (429.76 K, 3.296 kJ/mol) while for the heat capacity calibration, a sapphire sample was used and measured in the same conditions as the studied samples. The measurements were carried out using powder samples of ~15 mg. For the X = 3-Cl compound, the heat capacity measurements were carried out by AC calorimetry in the 5-300 K temperature range. In this case, the sample is a pressed pellet with a disc shape (3 mm of diameter, around 100 μm of thickness, and weighting ~1 mg). Using this technique, only relative heat capacity values are measured, and then absolute values are determined by scaling the data to the results obtained by DSC around room temperature.

Acknowledgements

This work was supported by the Spanish MICINN and FEDER, projects MAT2007-61621 and CSD2007-00010. The European Union Network of Excellence **MAGMANet** is also acknowledged.

References

[1] *Molecular Magnets : Recent Highlights* (Eds. W. Linert, M. Verdaguer), Springer, Wien, **2003**
[2] *Spin-Crossover in Transition Metal Compounds*, *Vols. I-II*, in *Topics in Current Chemistry* (Eds. P. Gutlich and H.A. Goodwin), Springer, Berlin, **2004**.
[3] S. Decurtins, P. Gütlich, C.P. Kölher, H. Spiering, A. Hauser, *Chem. Phys.* Lett. **1984**, *105*, 1.
[4] J.F. Létard, *J. Mat.Chem*. **2006**, *16*, 2550-2559 and references therein.
[5] P.Gütlich, Y. Garcia, H.A. Goodwin, *Chem. Soc. Rev.* **2000**, *29*, 419.
[6] J.A. Real, A.B. Gaspar, M.C. Muñoz, *Dalton Trans.,* **2005**, 2062.
[7] a) G. Dupouy, M. Marchivie, S. Triki, J. Sala-Pala, C.J. Gomez-Garcia, S. Pillet, C. Lecomte, J.F. Letard, Chem. Commun., **2009**, 3404-3406; b) S.M. Neville SM, B.A. Leita, G.J. Halder, C.J. Kepert, B. Moubaraki, J.F. Letard, K.S. Murray, *Chem. Eur. J.* **2008**, *14*, 10123-10133; c) A. Absmeier, M. Bartel, C. Carbonera, G.N.L. Jameson, P. Weinberger, A. Caneschi, K. Mereiter, J.F. Létard, W. Linert, *Chem. Eur. J*. **2006**, *12*, 2235-2243 ; d) V. Niel, A. Thompson, A.E. Goeta, C. Enachescu, A. Hauser, A. Galet, M.C. Muñoz, J.A. Real, *Chem. Eur. J.*, **2005,** *11*, 2047-2060 ; e) V. Niel, A. Galet, A.B. Gaspar, M.C. Muñoz, J.A. Real, Chem. Comm. **2003**, 1248.
[8] a) Y. García, V. Ksenofontov, P. Gütlich, *Hyperfine Interact.* **2002**, *139/140,* 543; b) S.B. Erenburg, N.V. Bausk, L.G.Lavrenova, L.N. Mazalov, *J.Magn. Magn. Mater.*, **2001**, *226*, 1967; c) X.J. Liu, Y. Morimoto, A. Nakamura, T. Hirao, S. Toyazaki, N. Kojima, *J. Phys. Soc. Jpn.*, **2001**, *70*, 2521; d) Y. García, V. Ksenofontov, G. Levchenko, G. Schmitt, P. Gütlich, *J. Phys. Chem. B.* **2000**, *104,* 5045; e) S.B. Erenburg, N.V. Bausk, L.G.Lavrenova, L.N. Mazalov, *J. synchr. Rad.*, **1999**, *6*, 576. f) K. Nakao, S. Hayami, M. Akita, K. Inoue, *Chem. Lett..,* **2008**, *37*, 292-293
[9] T. Kitazawa, Y. Gomi, M. Takahasi, M. Takeda, M. Enomoto, A. Miyazaki, T. Enoki, *J. Mater. Chem.*, **1996**, *6*, 119.
[10] a) T. Kitazawa, Mi. Takahasi, Ma. Takahasi, M. Enomoto, A. Miyazaki, T. Enoki, M. Takeda, *J. Radio. Anal. Nucl. Chem.,* **1999***, 239*, 285; b) T. Kitazawa, M. Eguchi, M. Takeda, *Mol. Cryst. Liq. Cryst.,* **2000**, *341,* 527; c) K. Hosoya, T. Kitazawa, M. Takahasi, M. Takeda, J.F. Meunier, G. Molnar, A. Bousseksou, *Phys. Chem. Chem. Phys.,* **2003**, *5,* 1682.
[11] G. Molnar, T. Kitazawa, L. Dubrovinsky, J.J. Mc Garvey, A. Bousseksou, *J. Phys. Condens. Matter,***2004**, *16,* 1129.
[12] G. Molnar, T. Guillon, N. Moussa, L. Rechignat, T. Kitazawa, M. Nardone, A. Bousseksou, *Chem. Phys. Lett.,***2006**, *423,* 152.
[13] A. Galet, M. C. Muñoz, A.B. Gaspar, J.A. Real, *Inorg. Chem.,* **2005**, *44,* 8749.
[14] a) A. Galet, M.C. Muñoz, V. Martínez, J.A. Real, *Chem. Commun.,* **2004**, 2268; b) A. Galet, V. Niel, M.C. Muñoz, J.A. Real, *J. Am. Chem. Soc.,* **2003**,*125*, 14224.
[15] S. Bonhommeau, G. Molnar, A. Galet, A. Zwick, J.A. Real, J.J. McGarvey, A. Bousseksou, *Angew. Chem. Int. Ed.* **2005**, *44,* 4069-4073
[16] V. Niel, J. M. Martínez-Agudo, M. C. Muñoz, A. B. Gaspar, J.A. Real, *Inorg. Chem.,* **2001***, 40,* 3838-3839.
[17] G. Agustí, S. Cobo, A.B. Gaspar, G. Molnár, N. O. Moussa, P.A. Szilágyi, V. Pálfi, C. Vieu, M.C. Muñoz, J.A. Real, A. Bousseksou, *Chem. Mater.,***2008**, *20*, 6721-6732.
[18] V. Niel, M.C. Muñoz, A. B. Gaspar, A. Galet, G. Levchenko, J.A. Real, *Chem. Eur. J.*,**2002**, *8,* 2446.
[19] J.A. Rodríguez-Velamazán, M. Castro, E. Palacios, R. Burriel, T. Kitazawa, T. Kawasaki, *J. Phys. Chem. B* **2007,** *111*, 1256-1261
[20] M. C. Muñoz, A.B. Gaspar, A. Galet, J.A. Real, *Inorg. Chem.,***2007**, *46*, 8182-8192.
[21] G. Agustí, M.C. Muñoz, A. B. Gaspar, J.A. Real, *Inorg. Chem.*, **2008**, *47*, 2552-2561.
[22] V. Martínez, A.B. Gaspar, M.C. Muñoz, G.V. Bukin,G. Levchenko, J.A. Real, *Chem. Eur. J.*, **2009,** *15*, 10960-10971
[23] a) K Nakano, N. Suemura, K. Yoneda, S. Kawata, S. Kaizaki, *Dalton Trans.* **2005**, 740. b) J.F. Letard, C. Carbonera, J.A. Real, S. Kawata,S. Kaizaki, *Chem. Eur. J.* **2009**, *15*, 4146 – 4155
[24] M. Sorai, *Top. Curr. Chem*. **2004,** *235*, 153.
[25] R. Boča, M. Boča, H. Ehrenberg, H. Fuess, W. Linert, F. Renz, I. Svoboda, *Chem. Phys.* **2003,** *293*, 375.
[26] J.A. Rodríguez-Velamazán, M. Castro, E. Palacios, R. Burriel, J.S. Costa, J.F. Létard, *Chem. Phys. Lett.* **2007**, *435*, 358
[27] C.P. Slichter, H.G. Drickamer*, J. Chem. Phys*., **1972**, *56*, 2142.
[28] P. Gütlich, H.A. Goodwin, *Top. Curr. Chem*. **2004,** *233*: 1.
[29] K.F. Purcell, M.P. Edwards*, Inorg. Chem*.,**1984**, *23*, 2620
[30] L. Capes, J.F. Létard, O. Kahn, *Chem. Eur. J.* **2000***, 6***,** 2246
[31] A. Hauser, *Top. Curr. Chem*. **2004,** *233*, 49.

[32].F. Létard, P. Guionneau, L. Rabardel, J.A.K. Howard, A.E. Goeta, D. Chasseau, O. Kahn, *Inorg. Chem*. **1998**, *37*, 4432
[33] A. Hauser, *Top. Curr. Chem*. **2004,** *233*, 49-58.
[34] G. S. Matouzenko, J.-F. Létard, S. Lecocq, A. Bousseksou, L. Capes, L. Salmon, M. Perrin, O. Kahn, A. Collet, *Eur. J. Inorg. Chem.* **2001**, 2935-2945.
[35] B.A. Leita, S.M. Neville, G.J. Halder, B. Moubaraki, C.J. Kepert, J.F. Letard, K.S. Murray, *Inorg. Chem.* **2007** *46*, 8784-8795
[36] C. Carbonera, A. Dei, C. Sangregorio, J.-F. Létard, *Chem. Phys.* Lett. **2004**, *396*, 198-201.
[37]V. Mishra, R. Mukherjee, J. Linares, C. Balde, C. Desplanches, J.F. Letard, E. Collet, L. Toupet, M. Castro, F. Varret, *Inorg. Chem.* **2008** *47*, 7577-7587
[38] Soma, T.; Iwamoto, T. *J. Incl. Phenom. Mol. Rec.*, **1996**, *26*, 161.
[39] C. Carbonera, A. Dei, C. Sangregorio, J.-F. Létard, *Chem. Phys. Lett.* **2004**, *396*, 198 –201.